Structural and Electrochemical Behaviour of Cucurbita Seed Like Zinc Oxide Nanoparticles by Chemical Reflux Route

R. Ranjithkumar, S. Ezhil Arasi, P. Devendran, N. Nallamuthu, P. Lakshmanan, M. Krishna Kumar

Abstract: Cucurbita seed like zinc oxide (ZnO) nanoparticle is synthesised via chemical reflux method. The phase, size and structure of ZnO elucidates by X-ray diffraction method. Infrared spectrum is revealed its functional groups which are present in the synthesised nanoparticles. The cucurbita seed like morphology of prepared zinc oxide nanoparticles were examined by SEM analysis. Optical absorption property and bandgap of synthesized ZnO nanoparticles are investigated. The electrochemical activity of Cucurbita seed like ZnO nanoparticles measurement carry out through electrochemical impedance analysis, galvanostatic charge discharge and cyclic voltammetry results.

Keywords : ZnO nanoparticle, chemical reflux method, cyclic voltammetry, electrochemical analysis.

I. INTRODUCTION

The energy production and storage has global research interest and concern in modern society, who owing gathering gadgets is in increasing demand [1]. It demonstrates a significant amount of attention must be provided to enhance the present energy storage systems to satisfy future modern devices. Various energy storage devices like, supercapacitors (Sps) which have the basic character of higher power density of high energy density. Lithium-ion batteries are considered as an appreciable candidate for increasing energy demand to higher energy storage purpose with low cost and eco-friendly [2]. This outstanding properties of hybrid energy materials generate modern commercial applications, i.e., hybrid electric vehicles, energy back-up devices, and other military electronic devices [3]. In particular, Sps can exhibit best

* Correspondence Author
  R. Ranjithkumar, Department of Physics, International Research Centre, Kalasalingam Academy of Research and Education,
  Krishnankoil – 626126. Tamil Nadu, India.
  S. Ezhil Arasi, Department of Physics, International Research Centre, Kalasalingam Academy of Research and Education,
  Krishnankoil – 626126. Tamil Nadu, India.
  P. Devendran, Department of Physics, International Research Centre, Kalasalingam Academy of Research and Education,
  Krishnankoil – 626126. Tamil Nadu, India.
  N. Nallamuthu, Department of Physics, International Research Centre, Kalasalingam Academy of Research and Education,
  Krishnankoil – 626126. Tamil Nadu, India.
  P. Lakshmanan, Department of Chemistry International Research Centre, Kalasalingam Academy of Research and Education, Krishnankoil – 626126,Tamil Nadu, India.
  M. Krishna Kumar* Department of Physics, International Research Centre, Kalasalingam Academy of Research and Education, Krishnankoil – 626126. Tamil Nadu, India. Email: m.krishnakumar@klu.ac.in

features to further investigate that others like quick responses of charge-discharge, long life. Also, it exhibits either a pseudocapacitor or electric double layer capacitor (EDLC), but nowadays hybrid capacitors are researched to exhibits mixed properties of both. Transition metal oxides (TMO) have great attention due to its superior performance and reliability in energy storage applications [4]. Various TMOs and hydroxides i.e., Ni(OH)2 [5], SnO_2 [6], RuO_2 [7], NiO [8], Co_3O_4 [9], Fe_3O_4 [10], MnO_2 [11], TiO_2 [12], MoO_3 [13], CuO [14] were studied for the electrode applications in energy storage devices. Zinc oxide (ZnO) is the most researched TMO for energy applications because of its great electrical conductivity σ=230 S/cm., but it has a higher hypothetical capacity of ~1000 mAh/g [15-18]. It is used as an anode material for supercapacitors to its various controlled morphologies [19-22]. But, in this research work, we aimed to get modified morphology by changing the synthesis environment from previous; we adopted the chemical route synthesis procedure and synthesized ZnO Nps. Its structural, spectral, linear optical and electrochemical results were measured and published in this article.

II. MATERIAL SYNTHESIS

A. ZnO nanoparticles via Chemical reflux route

$Zn(NO_3).6H_2O$ (0.02M) is added in 90 ml deionized water at the round bottom flask and separately NaOH (0.3g) aqueous solution (10ml) in beaker. It is added dropwise into $Zn(NO_3).6H_2O$ solution and stirred about 3 hrs to get homogenous reacted solution and ZnO Nps. The complete synthesis process is maintained at 120 ^oC to achieve uniform-sized ZnO nanoparticles and it may also depend on the reflux time and speed. Binding agent Hexamine (0.01M) is included in this solution to avoid removal of embedded ZnO nanoparticles. After 3 hrs precipitation of ZnO is gathered and washed in distilled water and ethanol to enrich the quality of synthesized material and it is dried at 80 ^oC for 10 hrs. These prepared ZnO nanoparticles are subjected to spectral, surface image and structural characterizations to evaluate its chemical and physical identity and electrode preparation for CV studies.

III. RESULTS AND DISCUSSION

A. Structural characterization

Diffracted X-ray pattern is collected for synthesized ZnO nanoparticles by using

D8 advanced ECO XRD instrument of SSD160 1D X-ray detector with Cu-Kα (1.5406 Å). Powder sample of ZnO is scanned from 10° to 80° with a scanning rate of 0.02° per sec. The obtained pattern of X-ray diffraction is shown in the Fig.1
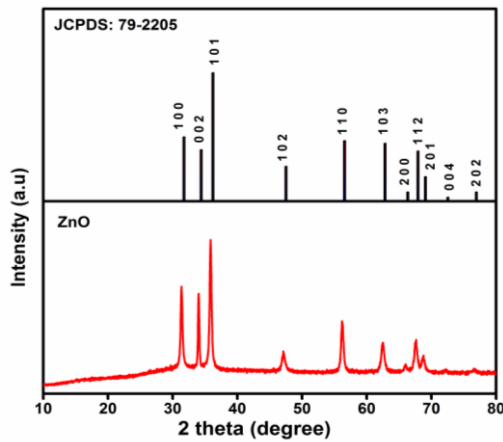

Fig. 1. XRD patterns of of ZnO nanoparticles

A very sharp peak dictates the synthesised sample is crystalline nature and exact matching of its (hkl) planes with JCPDS card [79-2205] data confirms it is hexagonal structured ZnO material [23] (Fig.1) and no additional peaks dictate its purity. The crystallite size was estimated theoretically by using from Debye–Scherrer formula,

$$D = k\lambda/\beta\cos\theta \ldots\ldots(1)$$

Where θ – angle of diffraction, β is the Full-Width and Half Maximum (FWHM) and k is the constant. The calculated average crystallite size is measured as 28.3 nm.
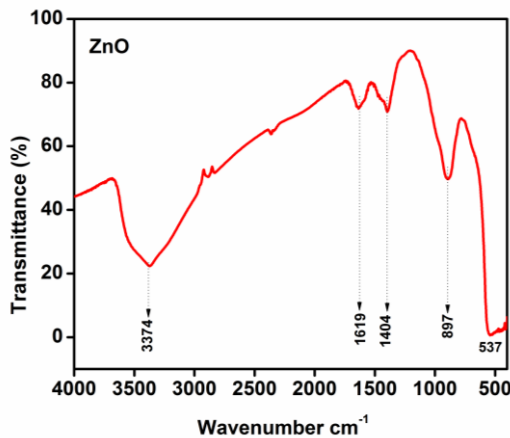
B. FTIR analysis

Fig. 2. FTIR spectrum of ZnO nanoparticle

The present functional groups, intra, inter-molecular vibrations and molecular interactions of prepared ZnO are examined through FT-IR spectra (Fig.2). It provides that, evidence to declare as ZnO. Shimadzu IR Trace-100 spectrometer instrument is utilized to record the FTIR spectra by the KBr pellet technique. The 400-4000cm⁻¹ range is recorded as shown in Fig.2. A broad vibrational band occurs at 3374 cm⁻¹, caused due to stretching of O-H bond. The vibrations wavenumbers at 1404cm⁻¹ and 1619 cm⁻¹ are interpreted due to C=O and O-H symmetrical vibrations

respectively [24]. The characteristic peaks of Zn-O molecule stretching band found at 537cm⁻¹. These characteristic peaks confirm that the prepared sample via chemical route synthesis is ZnO nanoparticles.

C. UV absorption property and Bandgap energy

The character of light absorption and important bandgap energy is calculated by using ultraviolet spectra, and it is recorded for the prepared ZnO nanoparticles. The ZnO nanoparticles are dispersed in 100ml de-ionized water and then sonicated about 10 minutes for the well-mixed solution of the study and it is used for the UV measurement at room temperature. Shimadzu 1800 model instrument was used for the experiment and spectra record in the range of 200nm-1100 nm as shown in the (Fig.3).
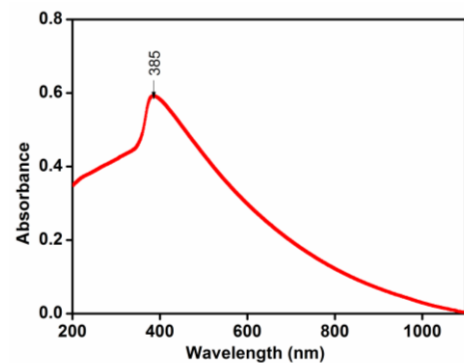

Fig. 3. UV- Vis spectrum of ZnO nanoparticle

The strong light absorption peak at 381nm was found in near semiconductor bandgap region. The optical energy band gap was calculated by using,

$$\text{Energy gap (Eg)} = h \ (c/ \ \lambda) \ldots\ldots(2)$$

Where, h = 6.626×10-34 J/ sec, c = 2.99×10⁸ m/sec, and λ = Absorption peak value and also 1eV = 1.6×10⁻¹⁹ J. The calculated band-gap of prepared ZnO nanoparticles via chemical route was 3.2eV, which is slightly lesser than bulk ZnO material (3.31eV). It may attributed to creation of oxygen vacancies at surface of ZnO nanoparticles [25].

D. Surface and Elemental analysis

The surface morphology of ZnO nano particle is shown in the Fig. 4(a). The SEM images closely matched with the pumpkin (Cucurbita) seed like structure. The surface morphology is shown in different magnifications 100nm, 200nm and 1µm. The electrochemical performance was depending on the structure of pumpkin seed like ZnO nanoparticle. It can be clearly seen that there were no agglomerations during growth process. In lower magnification the uniform formation of nanoparticles were found. From the figure 5 (a) EDS spectrum were shown. The atomic and weight percentage of prepared nanoparticles were obtained and elemental composition were determined. The presence of zinc and oxygen in desired composition were confirmed through EDS spectrum as shown in fig. 5.
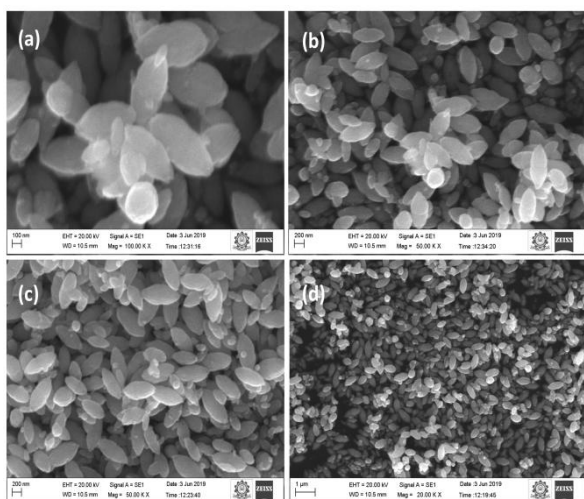
Fig. 4. Surface morphology of cucurbita seed like ZnO nanoparticles with different magnifications
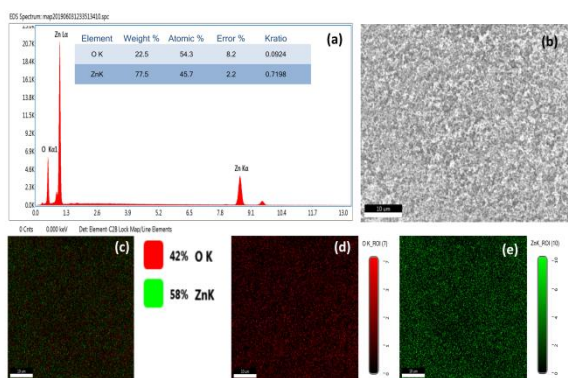

Fig. 5. Elemental conformations of ZnO nanoparticles

E. Electrochemical analysis

1) Cyclic voltammetry

The electrochemical reactions of prepared Zinc oxide nanoparticles via chemical synthesis route are examined in KOH (1M) electrolyte in three electrode electrochemical workstation (CHI6008 model). Nickel foil ($1cm^2$) is used as an electrode base to coat 0.01 mm thick cucurbita seed like ZnO nanoparticles sample. The surface of the foil was scoured via sandpaper and kept at sonication for cleaning and washed by $(CH_3)_2CO$. The calculated amount of 80wt% ZnO nanoparticles, 10wt% of activated carbon (AC) and 10wt% Polyvinylidene fluoride (PVDF) are mixed together and pounded well to mixing homogenously. Additionally, N-methyl-2-pyrrolidone (NMP) is mixed dropwise to the mixture to make it like glue and it is pasted on nickel foil as a thin film. Then, it is dried at 80^oC about 12hr. This, the working electrode is kept at 1M KOH electrolyte in CHI6008E model workstation, in which Platinum (Pt) act as auxiliary electrode and Ag/AgCl act the reference electrode.
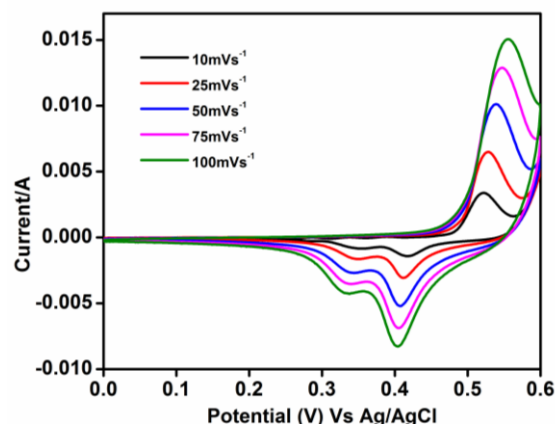

Fig. 6. Cyclic voltammetry curve of ZnO working electrode

Fig.6 shows that, ZnO Nps cyclic voltammetry curves in 0 to 0.6V potential range. The specific capacitance of the cucurbita seed like ZnO electrode is determined from the equation (3)

$$C_{sp} = \int IVdv/ mv\Delta V \ldots\ldots\ldots (3)$$

Where, $\int IVdv$ is the area of working electrode, 'm' is the mass of active material, 'v' is the scan rate and 'ΔV' is the potential window applied to the electrodes. CV is carried out for different scan rates (100 mVs^{-1} to 10 mVs^{-1}) to understand electrochemical property of this ZnO nanoparticles via its oxidation-reduction peaks. When the scanning rates were increased, the shape and area of the CV curves are increases with higher current but remains its actual position. The oxidation peak is occured between 0.3V and 0.4V of the applied voltage and the reduction peak is found at 0.55 V. The specific capacitance values are calculated as 61.6 F/g, 52.5 F/g, 45.7 F/g, 41 F/g and 37 F/g at different scan rates 100 mVs^{-1} to 10 mVs^{-1} respectively and it is depicted in Fig.7.

2) Galvanostatic charge and discharge

The galvanostatic charge and discharge characters were observed in the CV of three-electrode system between 0 to 0.55V at various current densities. The specific capacitance is calculated from following formula,

$$C_{sp} = It/ m \Delta V \ldots\ldots\ldots (4)$$

Where 'I' is the scanning current at the charge-discharge process,'t' is the electrode discharge time per second, 'm' is the mass of electrode material and 'ΔV' is the operating potential window.

Fig.8 displays, the charge and discharge arcs at a various current densities of ZnO electrode. The charge-discharge curve exhibits that, pseudocapacitance behaviour of ZnO electrode. The curves at higher current densities show the small internal resistance and drop occurs at 5 mA almost for all the curves.
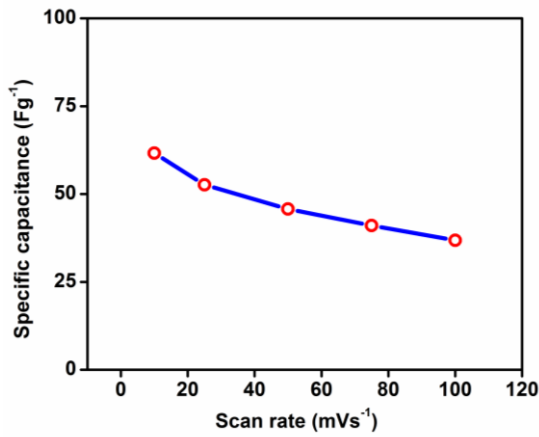
Fig. 7. Specific capacitances Vs Scan rate of cucurbita seed like ZnO nanoparticles
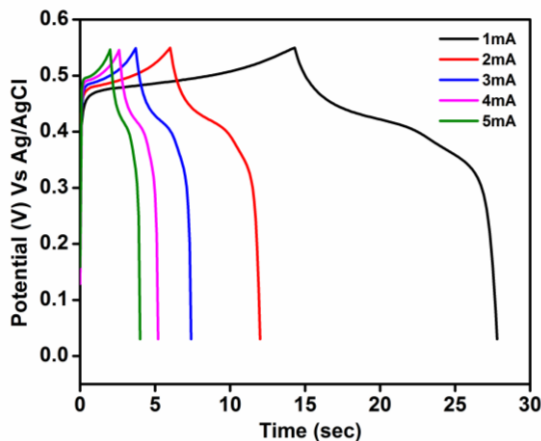

Fig. 8. Galvanostatic charge-discharge curve of cucurbita seed like ZnO nanoparticles coated electrode

The specific capacitance from the charge-discharge curves are 24 F/g, 21 F/g, 20 F/g, 18 F/g and 17 F/g for the different current densities of $1 mAs^{-1}$ to $5 mAs^{-1}$ respectively and it is depicted in Fig.9.
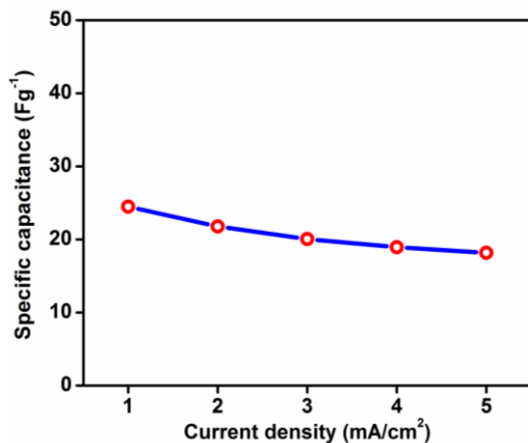

Fig. 9. Specific capacitance Vs Current density of ZnO electrode

3) Electrochemical impedance measurement

The Electrochemical Impedance Spectra (EIS) measurements remained taken in the frequency range of 0.01Hz to 1MHz. Nyquist plot of the ZnO electrode is shown in Fig.7. The impedance plot has three regions that are internal resistance, ohmic region and high frequency. The

high-frequency region shows the electrode and electrolyte interface. The mid-frequency region provides evidence about electron transfer resistance. The low-frequency region is an almost straight line and is relating to particle dispersion in electrode material during the electrochemical process.
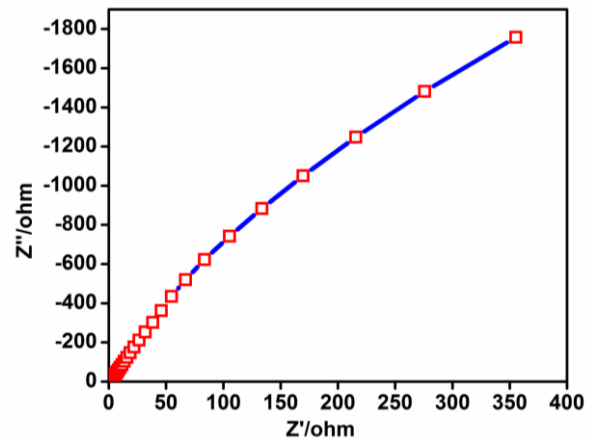

Fig. 10. Nyquist plot of ZnO electrode

The energy density vs power density is known as the Ragone plot and it is depicted in Fig.9. The ZnO nanoparticles are exhibited maximum deliverable of energy density (1Wh/kg) and power density (1386W/Kg) from 1M KOH electrolyte.
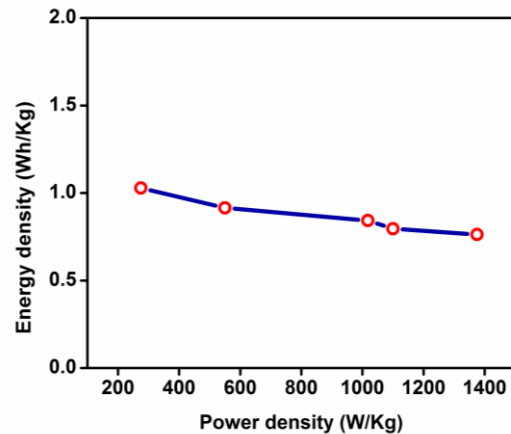

Fig. 11. Power density Vs Energy density Ragone plot of ZnO electrode.

IV. CONCLUSION

Zinc oxide nanoparticles were successfully synthesized via chemical synthesis route. The hexagonal structure of crystal is confirmed by JCPDS card [79-2205]. Infrared spectrum, too confirmed its composition with vibrational energies as expected. The optical absorption is found at 385 nm and bandgap was estimated as 3.2 eV. The specific capacitance value is calculated by using CV curves as 61.6 F/g at 10 mVs^{-1} scan rate. Electrochemical impedance spectra of the Nyquist plot of the ZnO electrode were analysed. The maximum deliverable of energy density (1Wh/kg) and power density (1386W/Kg) in 1M KOH electrolyte was found to the prepared ZnO nanoparticles made electrode, which is significant for the supercapacitor applications.

REFERENCES

1. Zhang, F., Zhang, T., Yang, X., Zhang, L., Leng, K., Huang, Y., & Chen, Y. energy storage device based on graphene-enhanced electrode materials with ultrahigh energy density . *Energy Environ. Sci.,* (2013) pp.1623–1632.
2. Kouchachvili, L., Yaïci, W., & Entchev, E. (2018). Hybrid battery/supercapacitor energy storage system for the electric vehicles. *Journal of Power Sources*, 374(October 2017), pp.237–248.
3. Z. Fan, J. Yan, T. Wei, L. Zhi, G. Ning, T. Li, F. Wei, Asymmetric supercapacitors based on graphene/MnO2 and activated carbon nanofiber electrodes with high power and energy density, *Adv. Funct. Mater.* 21 (2011)pp. 2366–2375.
4. E. Frackowiak, V. Khomendo, K. Jurewicz, K. Lota, F. Beguin, *Journal of Power Sources* Vol.153 (2006) pp413–418.
5. H. Niu, D. Zhou, X. Yang, X. Li, Q. Wang, F. Qu, Towards three-dimensional hierarchical ZnO nanofiber@Ni(OH)2 nanoflake core–shell heterostructures for high-performance asymmetric supercapacitors, *J. Mater. Chem. A* Vol. 3 (2015) pp.18413–18421.
6. Y. Liu, Y. Jiao, Z. Zhang, F. Qu, A. Umar, X. Wu, Hierarchical SnO2 nanostructures made of intermingled ultrathin nanosheets for environmental remediation, smart gas sensor, and supercapacitor applications, *ACS Appl. Mater. Interfaces* 6 (2014) pp.2174–2184.
7. R.B. Rakhi, W. Chen, M.N. Hedhili, D. Cha, H.N. Alshareef, Enhanced rate performance of mesoporous Co3O4 nanosheet supercapacitor electrodes by hydrous RuO2 nanoparticle decoration, *ACS Appl. Mater. Interfaces* 6 (2014) pp.4196–4206.
8. P. Anjali, T.S. Sonia, I. Shakir, S.V. Nair, A. Balakrishnan, On the synthesis and electrochemical characterization of ordered hierarchical NiO micro bouquets with trimodal pore size distribution, *J. Alloys Compd.* 618 (2015) pp.396–402.
9. B. Wang, Y. Wang, J. Park, H. Ahn, G. Wang, In situ synthesis of Co3O4/graphene nanocomposite material for lithium-ion batteries and supercapacitors with high capacity and supercapacitance*, J. Alloys Compd.* 509 (2011) pp.7778–7783.
10. V.A. Online, M. Liu, J. Sun, In situ growth of monodisperse Fe3O4 nanoparticles on graphene as flexible paper for supercapacitor, *J. Mater. Chem. A* 2 (2014) pp.12068–12074.
11. P. Yang, Y. Ding, Z. Lin, Z. Chen, Y. Li, P. Qiang, M. Ebrahimi, W. Mai, C.P. Wong, Z.L. Wang, Low-cost high-performance solid-state asymmetric supercapacitors based on MnO2 nanowires and Fe2O3 nanotubes, Nano Lett. 14 (2014) pp.731–736.
12. J. Xu, H. Wu, L. Lu, S.F. Leung, D. Chen, X. Chen, Z. Fan, G. Shen, D. Li, Integrated photo-supercapacitor based on Bi-polar TiO2 nanotube arrays with selective one-side plasma-assisted hydrogenation, *Adv. Funct. Mater.* 24 (2014) pp.1840–1846.
13. D. Hanlon, C. Backes, T. Higgins, J.M. Hughes, O. Neill, P. King, N. McEvoy, G.S. Duesberg, B.M. Sanchez, H. Pettersson, V. Nicolosi, J.N. Coleman, Production of molybdenum trioxide nanosheets by liquid exfoliation and their application in high performance supercapacitors, *Chem. Mater.* 26 (2014) pp.1751–1763.
14. M.J. Deng, C.C. Wang, P.-J. Ho, C.M. Lin, J.-M. Chen, K.T. Lu, Facile electrochemical synthesis of 3D nano-architectured CuO electrodes for high-performance supercapacitors, *J. Mater. Chem. A* 2 (2014) pp.12857–12865.
15. X. Li, Z. Wang, Y. Qiu, Q. Pan, P. Hu, 3D graphene/ZnO nanorods composite networks as supercapacitor electrodes*, J. Alloys Compd.* 620 (2015) pp.31–37.
16. S. Shi, X. Zhuang, B. Cheng, X. Wang, Solution blowing of ZnO nanoflakes-encapsulated carbon nanofibers as electrode for supercapacitor*, J. Mater. Chem. A* 1 (2013) pp.13779–13788.
17. J. Ding, M. Wang, J. Deng, W. Gao, Z. Yang, C. Ran, X. Zhang, A comparison study between ZnO nanorods coated with graphene oxide and reduced graphene oxide, *J. Alloys Compd.* 582 (2014) pp.29–32
18. X. Xiao, B. Han, G. Chen, L. Wang, Y. Wang, Preparation and electrochemical performances of carbon sphere@ZnO core–shell nanocomposites for supercapacitor applications, *Sci. Rep.* 7 (2017) 40167.
19. D. Kalpana, K.S. Omkumar, S.S. Kumar, N.G. Renganathan, A novel high power symmetric ZnO/carbon aerogel composite electrode for electrochemical supercapacitor, *Electrochim. Acta* 52 (2006) pp.1309–1315.
20. Y. Li, X. Liu, Activated carbon/ZnO composites prepared using hydrochars as intermediate and their electrochemical performance in supercapacitor, *Mater. Chem. Phys.* 148 (2014) pp.380–386.
21. G. Du, Y. Li, L. Zhang, X. Wang, P. Liu, Y. Feng, X. Sun, Facile self-assembly of honeycomb ZnO particles decorated reduced graphene oxide, *Mater. Lett.* 128 (2014) pp.242–244.
22. Z. Zhang, L. Ren, W. Han, L. Meng, X. Wei, X. Qi, et al., One-pot electrodeposition synthesis of ZnO/graphene composite and its use as binder-free electrode for supercapacitor, *Ceram. Int.* 41 (2015) pp.4374–4380.
23. R. Ranjithkumar, S. Ezhil Arasi, S. Sudhahar, N. Nallamuthu, P. Devendran, P. Lakshmanan, M. Krishna Kumar, Enhanced electrochemical studies of ZnO–CNT nanocomposite for supercapacitor devices, *Physica B* Vol.568 (2019) pp.51-59.
24. Brian Smith, Infrared Spectral Interpretation: A Systematic Approach, First ed., *CRC press*, (1999).
25. C. Aydın, M.S. Abd El-sadek, K. Zheng, I.S. Yahia, F. Yakuphanoglu, Synthesis, diffused reflectance and electrical properties of nanocrystalline Fe-doped ZnO via sol–gel calcination technique, Opt. *Laser Technol.* 48 (2013) pp 447–452.